Gradient-based optimization of a 15 MW wind turbine spar floater

Pollini, Nicolò; Pegalajar-Jurado, Antonio; Dou, Suguang; Bredmose, Henrik; Stolpe, Mathias

Published in:
Journal of Physics: Conference Series

Link to article, DOI:
10.1088/1742-6596/2018/1/012032

Publication date:
2021

Document Version
Publisher's PDF, also known as Version of record

Gradient-based optimization of a 15 MW wind turbine spar floater

Gradient-based optimization of a 15 MW wind turbine spar floater

Nicolò Pollini[1], Antonio Pegalajar-Jurado[2], Suguang Dou[1], Henrik Bredmose[2], Mathias Stolpe[1]

[1] Technical University of Denmark, Department of Wind Energy, Frederiksborgvej 399, 4000 Roskilde, Denmark
[2] Technical University of Denmark, Department of Wind Energy, Nils Koppels Allé, 2800 Kgs. Lyngby, Denmark

E-mail: nipol@dtu.dk, ampj@dtu.dk, sudou@dtu.dk, hbre@dtu.dk, matst@dtu.dk

Abstract. We discuss the optimization-based conceptual design of support structures and mooring system for floating wind turbines. A four degree-of-freedom frequency-domain model is used for the dynamic response of a spar floating wind turbine subjected to wind and wave loads. The framework allows for design optimization involving the geometrical properties of the floater and the mooring system and inclusion of long realizations of multiple load cases in the analysis. The adopted optimization approach adopted relies on analytical design sensitivities of the governing frequency-domain equations and of the design requirements. This ensures that modern gradient-based optimization algorithms can effectively be used to solve the design problem at hand. The optimization approach is applied to the design of the spar-buoy floater and its mooring system for the IEA 15 MW reference wind turbine. A post-processing approach for identifying discrete designs from predefined catalogues is also presented. The post-processing allows to transform continuous design solutions into practical ones that can be used in subsequent analyses with time domain response models for the full validation of the design solutions obtained. The numerical results highlight the capability of the approach discussed herein to provide discrete optimized designs for given design constraints and loads in few minutes requiring modest computational resources and time.

1. Introduction

Much of the offshore wind resource potential in the United States, China, Japan, Norway, and other countries is available in water deeper than 30 m [1]. However, to date most of the European offshore wind turbines are installed in shallow water, on monopile, jacket, or gravity-based substructures. Space-frame support structures (e.g. jackets) can push the installation of offshore wind turbines to deeper water up to approximately 60 m. At some depth, however, floating support platforms are the most economical. Floating wind turbines are complex multidisciplinary systems, and their design is a challenging and time-consuming task. The floating wind industry is still in the early stages of development, and floating wind turbines have already attracted significant attention from the research community. Most of the attention has been directed towards the development, analysis and testing of innovative floating support structures [2, 3, 4, 5, 6, 7]. In this work, we discuss the optimization-based design of the support structure for a reference 15 MW floating wind turbine [8], where the mooring system is also simultaneously optimized. The results presented herein contribute to the study

of highly performing design solutions for the support structures of floating wind turbines. The optimization problem is efficiently solved by Sequential Quadratic Programming (SQP) based on analytical gradients of the objective function and of the response constraint functions.

In previous work by Dou et al. [6], a four degree-of-freedom (DoF) model was used for the optimization-based conceptual design of a spar buoy for a 10 MW floating wind turbine. The floating wind turbine was subjected to pre-computed aerodynamic loads and linear hydrodynamic loads, with constraints on the system static and dynamic responses. A linearized mooring system was considered, represented by a stiffness matrix. A similar approach, with further extension to optimal control parameters, has very recently been presented by Hegseth et al. [7], which confirms the relevance of the Dou et al. approach. Herein, building on the framework presented in [6], we discuss an additional contribution in the context of optimization of floating wind turbine support structures. We present the first optimization-based design of a steel spar-buoy for a 15 MW reference wind turbine. A gradient-based optimization framework is utilized, which ensures that modern numerical optimization methods that rely on first-order information can efficiently be used to solve the design problem at hand. The wave loading on the offshore turbine is computed by the Morison equation. The aerodynamic loads and damping are pre-computed in FAST [9], which, for a given wind turbine, are extracted only once for each mean wind speed from time-domain aero-elastic rotor computations. These aerodynamic properties of forcing and linear damping are thus assumed to be independent of the design variables for the floater and mooring system. Lastly, we present a procedure aimed at translating the continuous designs obtained into discrete design solutions. This post-processing phase consists of two steps. In the first step we round the continuous solution obtained using the SQP algorithm to the nearest entries from predefined catalogues by solving a Mixed Integer Linear Programming problem (MILP). In the second step we use a heuristic local search algorithm inspired by the Relaxation Induced Neighborhood Search (RINS) presented by Danna et al. [10] with the purpose of improving locally, if possible, the solution obtained after rounding.

2. Modelling and analysis

We present in brief the details of the three systems of equations adopted to describe the response of the floating wind turbine considered, and of the associated mooring system. In particular, we consider the following systems of equations: the equations of motion in the frequency domain; the equations for the system eigenvalues; and the equations for the static response.

The floating wind turbine model, QuLAF [11], is the same as in [6], now adapted to the 15 MW turbine and with frequency-dependent aerodynamic damping. QuLAF has been extensively compared to FAST in previous work [11, 12], and generally a good agreement was found for the damage-equivalent bending moment at the tower base. The floater motion was also well estimated, with some under-prediction for strong sea states.

In the model, the system has four degrees of freedom, namely the floater surge, heave and pitch, and the first tower fore-aft bending mode. The wind turbine response is evaluated for wind and wave loads. The aerodynamic loads and damping are pre-computed. For a given wind turbine they are extracted only once for each mean wind speed from time-domain aero-elastic rotor computations. The aerodynamic properties are thus assumed to be independent of the design variables for the floater and mooring system. Linear hydrodynamic loads based on the Morison equation [13] are considered in this work. They are formulated in an efficient transfer-function format to speed up the optimization framework. The added mass is frequency-independent and Morison-based, and radiation damping is excluded. Viscous damping effects are included through a damping matrix, but viscous excitation is not included due to the loads being inertia-dominated.

2.1. Governing equations

The linear equations of motion in the frequency domain for a floating wind turbine are written as follows:

$$\left(-\omega^2(\mathbf{M}(\mathbf{v})+\mathbf{A}(\mathbf{v}))+i\omega\mathbf{B}(\mathbf{v})+\mathbf{C}(\mathbf{v})\right)\hat{\boldsymbol{\xi}}_j(\omega)=\hat{\mathbf{F}}_j^h(v,\omega)+\hat{\mathbf{F}}_j^a(\omega). \tag{1}$$

In Eq. (1), $\mathbf{v}$ is the vector of the design variables which include the geometric properties of the floater and the mooring system; $\hat{\boldsymbol{\xi}}_j(\omega)$ is the vector of the Fourier motion amplitudes in the frequency domain associated to the j-th environmental condition; and $\hat{\mathbf{F}}_j^h(v,\omega)$ and $\hat{\mathbf{F}}_j^a(\omega)$ are the hydrodynamic and aerodynamic loads in the frequency domain. The hydrodynamic loads are computed internally by means of the Morison equation for each design update and environmental condition. The aerodynamic loads are precomputed beforehand externally in FAST [9] considering rigid-structure rotor computations, hence they do not depend on the design updates. $\mathbf{M}(\mathbf{v})$ and $\mathbf{A}(\mathbf{v})$ are the structural mass and hydrodynamic added mass matrices, which are computed internally and updated during the optimization process; the damping matrix $\mathbf{B}(\mathbf{v})$ accounts for contributions from the tower structural damping, the aerodynamic damping, and the hydrodynamic viscous damping, which is computed internally for each design update; $\mathbf{C}(\mathbf{v})$ is the restoring matrix, which includes the hydrostatic and mooring contributions and it is recomputed after every design update during the optimization analysis.

We consider constraints limiting the dynamic response of the system. To this end, we constraint the maximum pitch motion in time θ_j^{dyn} of the floater for the j-th environmental condition. We approximate θ_j^{dyn} by the mean pitch plus three times its standard deviation, i.e. $\theta_j^{dyn}\cong\theta_{j,mean}^{dyn}+3\,\sigma_{j,\theta}$. Moreover, we constraint also the maximum nacelle acceleration in time a_j^{dyn} for each j-th environmental condition, approximated similarly to the maximum pitch as $a_j^{dyn}\cong 3\,\sigma_{j,a}$.

The optimization problem formulation considers also limits on the system eigenvalues, λ_i. They depend on the design variables and they are calculated from the following system:

$$(\mathbf{C}(\mathbf{v})-\lambda_i\,(\mathbf{M}(\mathbf{v})+\mathbf{A}(\mathbf{v})))\boldsymbol{\phi}_i=\mathbf{0}, \tag{2}$$

where $\boldsymbol{\phi}_i$ are the eigenmodes associated to the eigenvalues λ_i.

The static pitch and surge ($\mathbf{u}_s=[\theta_{stat}\ \ u_{stat}]^T$) are also constrained in the optimization problem formulation. They are calculated considering the rated thrust and its associated moment at the point of flotation, collected in the static load vector $\mathbf{f}_s$. The static pitch and surge are calculated by solving the following linear system:

$$\mathbf{C}_s(\mathbf{v})\mathbf{u}_s=\mathbf{f}_s \tag{3}$$

where $\mathbf{C}_s$ is the restoring matrix associated to the pitch and surge degrees of freedom.

2.2. Mooring system

We consider a mooring system made of three identical catenary lines and uniformly distributed along the circumference of the floater, represented by a stiffness matrix. The work by Al-Solihat and Nahon [14] provides an analytical derivation of the stiffness matrix for such a mooring system. Building on the framework presented in [6], analytical design sensitivities of the mooring stiffness matrix are adopted in the optimization code.

3. Optimization-based design approach

A schematic view of the type of spar-buoy floaters and the coupled mooring systems optimized in this work is shown in Fig. 1. In particular, we consider N design variables, where $N=6$ in

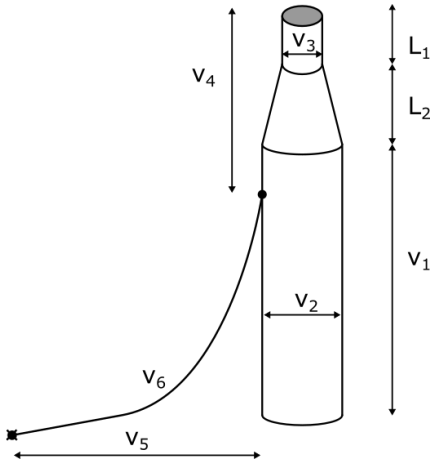

Figure 1. Schematic illustration of the spar buoy and mooring system optimized. Note that the conical section is simplified to a straight cylinder in the model.

the numerical experiments (see Fig. 1 for visual reference):

$$\mathbf{v} = \begin{bmatrix} v_1 & \text{length of main cylinder} \\ v_2 & \text{diameter of spar body} \\ v_3 & \text{diameter of spar head} \\ v_4 & \text{depth of fairlead} \\ v_5 & \text{anchor radius} \\ v_6 & \text{mooring line length} \end{bmatrix} \tag{4}$$

The optimization approach adopted herein consists of three steps. In the first step a continuous optimized design of a floater and the associated mooring system is obtained as in [6]. In the second stage the continuous design is rounded so that for each design variable the closest entries from a catalogue are chosen. In this step a MILP problem is solved to global optimality. The design obtained in the 2^{nd} step is further improved by means of a local search heuristic that explores the neighbored entries in the catalogue for each variable and updates the design accordingly if the new solution reduces the cost and satisfies all of the constraints. Essentially steps 2 and 3 can be seen as a post-processing phase of the initial continuous optimized design used to translate the initial solution into an engineering practical solution. In practice, the interpretation of the continuous optimized design is typically done based on engineering intuition, but in this way the optimality of the designs attained may be spoiled, or it may be unclear which specific strategy to follow in order to transform a continuous solution into a practical and discrete one. Here we propose an approach that automates this task instead, and it is discussed in the following.

3.1. Continuous optimization problem formulation

The optimization problem considered in the first step resembles the one discussed in [6] and it is here recalled briefly for the sake of clarity. The only difference consists of two additional constraints added here between the diameters of the spar body and head, in Eq. (6). These new constraints are added to avoid distorted shapes of the tapered part of the floater. The continuous optimization problem discussed in the following is a nonlinear and non-convex optimization problem. It consists in minimizing a mass-proportional objective cost function, which accounts for the costs associated to the floater, the ballast, and the mooring system. Constraints are

imposed on the eigenvalues, the dynamic and static response of the floating wind turbines considered. Formally, the optimization problem is stated as follows:

$$\begin{array}{lllll} \underset{\mathbf{v}\in\mathcal{F}}{\text{minimize}} & c(\mathbf{v}) & & & \text{(cost)} \\ \text{subject to} & \lambda_i^{min} \le \lambda_i(\mathbf{v}) \le \lambda_i^{max} & \forall i & & \text{(frequencies)} \\ & \theta_{dyn,j}(\mathbf{v}) \le \theta_{dyn}^{max} & \forall j & & \text{(dynamic pitch)} \\ & a_{dyn,j}(\mathbf{v}) \le a_{dyn}^{max} & \forall j & & \text{(tower top acceleration)} \\ & \theta_{stat}(\mathbf{v}) \le \theta_{stat}^{max} & & & \text{(static pitch)} \\ & u_{stat}(\mathbf{v}) \le u_{stat}^{max} & & & \text{(static surge)} \\ & v_k^{min} \le v_k \le v_k^{max} & \forall k & & \text{(bounds)} \end{array} \tag{5}$$

Here i is an index that runs over the eigenvalues constrained (in the numerical examples discussed here $i \in \{1,2,3\}$); j is an index that runs over the environmental conditions considered and that are listed in Table 1; and k is an index that runs over the design variables considered, $k \in \{1,\dots,N\}$. More details regarding the constraints upper and lower bounds are provided in Table 2. Additional constraints that do not require analyses in the frequency domain are collected in the set $\mathcal{F}$:

$$\mathcal{F} = \left\{ \begin{array}{ll} \mathbf{v} \mid z_b(\mathbf{v}) \ge z_{cm}(\mathbf{v}), & \text{(buoyancy center)} \\ l_m^{min} \le l_m(\mathbf{v}) \le l_m^{max}, & \text{(mooring line length)} \\ V_m(\mathbf{v}) \le \eta w_m(\mathbf{v}), & \text{(vertical force at the fairlead)} \\ \bar{v}_{23}\, v_2 \le v_3 \le v_2 & \text{(spar body/head diameters)} \end{array} \right\}, \tag{6}$$

where z_b is the buoyancy center of the floater and z_{cm} is the center of mass of the entire system; V_m is the vertical force at the fairlead and w_m is the weight in water of the mooring line; v_2 and v_3 are the diameters of the spar body and head and their ratio is constrained between $\bar{v}_{23}$ and 1 in order to ensure a desired shape of the tapered section of the floater.

The optimization analysis for the solution of (5) was implemented in MATLAB ver. 9.8.0. For optimization, we used the SQP algorithm implemented in the `fmincon` function, which is part of the MATLAB Optimization Toolbox ver. 8.5. The analytical gradients of the objective function and the constraints are implemented in the code and passed to the `fmincon` function. The analytical gradients have been validated against the gradients obtained with a finite-difference scheme, and more details can be found in [6].

3.2. Post-processing of the design

In the second step of the optimization approach, the goal is to round the optimized design solution obtained from Eq. (5), namely $\mathbf{v}^*$, to the nearest entries from predefined catalogues $\mathcal{V}_k$, with $k = 1,\dots,N$. The goal is to obtain a discrete solution while satisfying the general linear constraints as well as the requirements $v_k \in \mathcal{V}_k$ while ignoring the nonlinear constraints on the system static and dynamic response. This can be achieved in several different ways. We propose to solve the problem

$$\begin{array}{ll} \underset{\mathbf{x}\in\mathcal{X}}{\text{minimize}} & \|\mathbf{v} - \mathbf{v}^*\|_1 \\ \text{subject to} & \mathbf{A}\mathbf{v} \le \mathbf{b} \\ & \mathbf{v} = \mathbf{V}\mathbf{x} \end{array} \tag{7}$$

where $\mathbf{A}\mathbf{v} \le \mathbf{b}$ is the set of linear constraints that are retained from (5) for the mooring line length and spar-buoy diameters, and

$$\mathcal{X} = \left\{ \mathbf{x} \mid x_{kj} = \{0,1\},\ v_k = \sum_j V_{kj}\, x_{kj},\ \sum_j x_{kj} = 1 \right\} \tag{8}$$

where V_{kj} is the j-th entry in the catalogue for the k-th variable. The catalogue for each design variable is

$$\mathcal{V}_k = \{v_k^{min} : \Delta v_k : v_k^{max}\}, \quad k = 1, \ldots, N \tag{9}$$

More details regarding the catalogues considered in the numerical examples are given in Table 4. The problem (7) can, after applying suitable reformulation techniques, be cast as a mixed $0-1$ linear problem and thus solved to global optimality by branch-and-cut type algorithms [15] implemented in commercial software such as Gurobi Optimizer [16]. If the problem is feasible we can expect that the solver returns an optimal solution $\hat{\mathbf{v}}$.

In the third and last step of the optimization approach proposed, we search among points in the catalogues that are close to the point $\hat{\mathbf{v}}$. The chosen heuristic scheme adopted in inspired by the RINS approach presented by Danna et al. [10]. The heuristic modifies one variable at the time by moving it to the nearest value in the catalogue. It accepts the new design as the new incumbent if it reduces the cost while satisfying all of the constraints defined in the first optimization step, i.e. Eq. (5). The algorithm loops over all the variables one at the time and for all incumbents, until no further improvement in the design is found. The outcome of the third and last step is the discrete design $\bar{\mathbf{v}}$.

4. Numerical applications

In the following numerical applications we consider for optimization the IEA 15 MW reference wind turbine [8]. The tower design adopted is the one developed for the UMaine VolturnUS-S reference platform [17]. The water depth is 320 m. Twelve environmental conditions (ECs) are considered, and they are representative of Design Load Case (DLC) 1.2 for a wind turbine operating in normal conditions in a Gran Canaria site [18]. They are defined by a mean wind speed WS, a significant wave height H_s, and a wave peak period T_p, and listed in Table 1. The turbulent wind corresponds to a Kaimal spectrum, Class A and normal turbulence, and the irregular sea states are defined through a Pierson-Moskowitz spectrum. Each EC in Table 1 is simulated for one hour.

Table 1. Environmental conditions with wind speed (WS) in m/s, the significant wave height H_s in m, and the peak period T_p in s

EC	1	2	3	4	5	6	7	8	9	10	11	12
WS	5.00	7.00	9.00	10.59	11.00	13.00	15.00	17.00	19.00	21.00	23.00	25.00
H_s	1.00	1.36	1.72	2.00	2.09	2.52	2.95	3.38	3.82	4.25	4.68	5.11
T_p	5.00	5.36	5.72	6.00	6.09	6.50	6.92	7.33	7.75	8.17	8.58	9.00

In the numerical examples discussed in this section a spar-buoy floater anchored with three equally spaced catenary mooring lines is optimized. The geometry and the definition of the design variables are illustrated in Fig. 1 and Eq. (4). Following [6], the thickness of the steel tubes of the floater is fixed and set to 0.06 m. The mooring line effective mass in water is set to 300 kg/m. The price for steel and the mooring lines is set to 2.5 €/kg and 40.0 €/m, respectively. The price for ballast is set to zero. Clearly these parameters are predefined, and can be changed by the user if needed. The density of steel, ballast and water is set to 7850, 2600 and 1025 kg/m^3, respectively. The constraints for the optimal design problem and their limits are described in Table 1. The limits and the optimized values of the design variables are shown in Table 2, where for comparison the details of the WindCrete concrete spar floater [18] are also

listed. It should be noted that in the Gran Canaria site, for which the WindCrete concrete spar was designed, the water depth considered is 200 m. Here instead we consider a water depth of 320 m. The values of the catalogues considered in the second and third optimization steps described in Sec. 3.2 are listed in Table 4.

Table 2. List of constraints in the optimization problem for the spar-buoy floater (Eq. (5))

Type	Number	Description	Values
Stability	1	buoyancy center higher than mass center	0 (min)
Static response	2	maximum pitch angle (θ_{stat}^{max}) maximum surge (u_{stat}^{max})	8 ° 50 m
System periods	5	minimum surge period (T_1^{min}) min/max heave/pitch periods ($T_i^{min}, T_i^{max}, i = 2, 3$)	80 s 25, 40 s
Mooring line	3	min/max mooring line length v_6 maximum percentage of suspended line (η)	l_m^{min}, l_m^{max} 75%
Spar head diameter	2	minimum value $v_2\, 2\, h_{taper}\, \tan(\alpha^{max})$ maximum $v_2\, -\epsilon$	$\alpha^{max} = 30°$ 0.1
Dynamic response	24	maximum pitch angle (θ_{dyn}^{max}) maximum nacelle acceleration (a_{dyn}^{max})	10 ° 0.2 g

Table 3. Limits, initial and optimized values of the design variables in the first optimization step (Eq. (5)), where the SQP algorithm is used. For comparison, the details of the WindCrete spar floater [18] are also listed

Variables	Min	Max	Initial	Optimized 13 constraints	Optimized 37 constraints	WindCrete spar
Main cylinder length v_1 $[m]$	60	180	130	110.643	110.643	135.700
Spar diameter v_2 $[m]$	5	18	15	18.000	18.000	18.600
Spar head diameter v_3 $[m]$	5	18	10	9.427	9.427	13.200
Fairlead position v_4 $[m]$	-160	-12	-50	-12.000	-12.000	-90
Anchor radius v_5 $[m]$	600	1000	650	727.949	727.949	600.000
Mooring line length v_6 $[m]$	600	1100	750	826.650	826.650	565.000*

*There is an additional delta connection of 50 m.

Table 4. Catalogue of values used for the post processing of the optimized continuous design

	v_1	v_2	v_3	v_4	v_5	v_6
Minimum v_k^{min} $[m]$	60	5	5	-160	600	600
Step Δv_k $[m]$	1.0	0.5	0.5	0.5	1.0	1.0
Maximum v_k^{max} $[m]$	180	20	20	-12	2000	2100

The results obtained with and without the dynamic constraints on the maximum pitch and nacelle acceleration are identical and they are listed in Table 5. The only difference is in terms of computational time. When the dynamic constraints are considered, additional constraints are added to the optimization problem. These additional constraints require the evaluation of the dynamic system response in the frequency domain for the selected environmental conditions, and as a consequence the computational cost increases.

As it has been already observed, the optimized designs obtained in the two cases after the post-processing are basically identical. This is due to the fact that the governing constraints are

Table 5. Solutions obtained with/without dynamic constraints. The two solutions are identical

Optimization step	v_1 $[m]$	v_2 $[m]$	v_3 $[m]$	v_4 $[m]$	v_5 $[m]$	v_6 $[m]$	Cost (10^6 \$)	Computational time with/without dynamic constraints
0) Initial	130.000	15.000	10.000	-50.000	650.000	750.000	8.3414	N/A
1) SQP	110.643	18.000	9.427	-12.000	727.949	826.650	8.5044	15 m 11 s, 58 s
2) Rounding	111.000	18.000	9.500	-12.000	728.000	827.000	8.5343	0.18 s, 0.14 s
3) Local search	111.000	18.000	9.500	-12.000	728.000	824.000	8.5339	4 m 58 s, 18 s

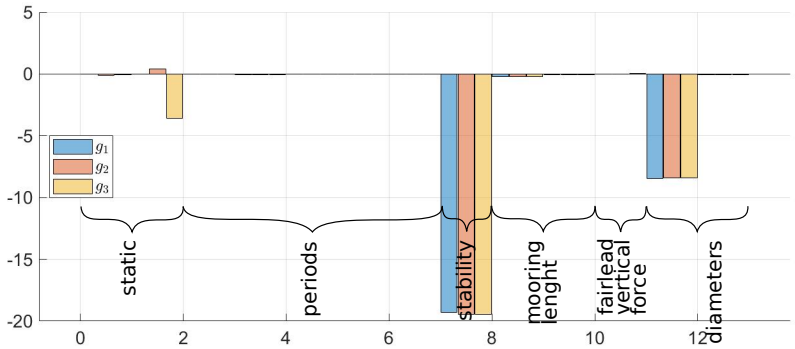

Figure 2. Values of the constraints in correspondence of the optimized design obtained without considering the dynamic constraints. For negative values, the constraints are satisfied

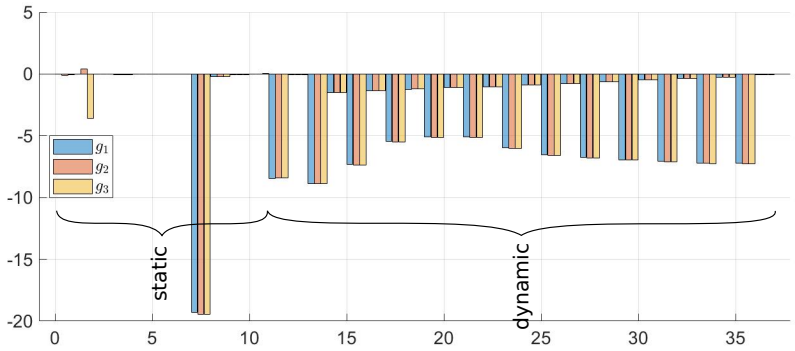

Figure 3. Values of the constraints in correspondence of the optimized design obtained considering also the dynamic constraints. For negative values, the constraints are satisfied

the static ones. Namely, these are the constraints on the static surge and pitch, the constraints on the system frequencies, and the constraints on the mooring force at the fairlead. This can be observed in Fig. 2 and Fig. 3, where in both cases the values of the static constraints in correspondence of the optimized designs tend to zero, i.e. they are active and hence governing the design. Moreover, Fig. 2 and Fig. 3 show also that in both cases the post-processing phase successfully identify discrete conceptual design solutions (listed in Table 5) that can be used "as is" for further analyses with higher-fidelity models. Fig. 2 and Fig. 3 show also that when solving problem (7) one constraint is significantly positive, i.e. it is violated. This happens in the rounding post-processing step, because in Eq. (7) no information on the system response is retained and hence constrained. However in the third step the heuristic search algorithm successfully further improves the solution satisfying also all of the response constraints within acceptable tolerances.

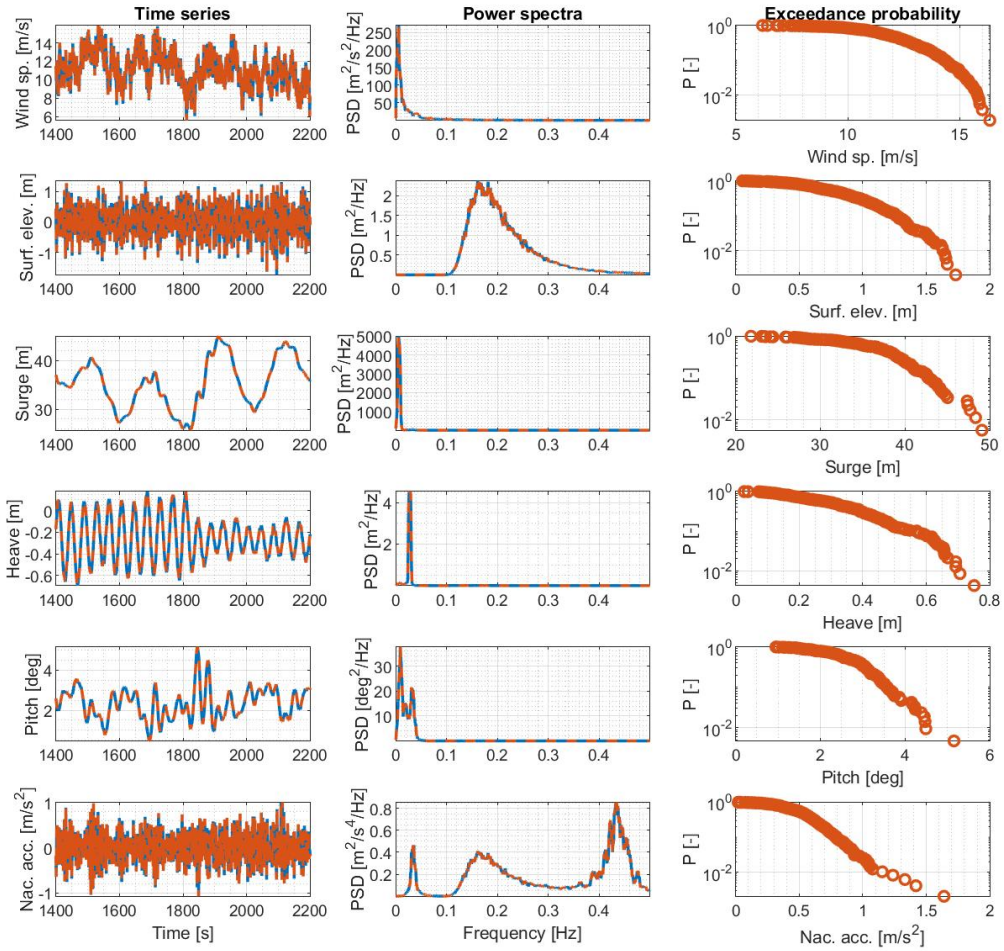

Figure 4. Comparison of the dynamic responses at rated wind speed of the optimized design with (in blue) and without (in red) inclusion of the dynamic constraints. The mean wind speed is 10.59 m/s, significant wave height is 2.00 m, and the wave peak period is 6.00 s

The dynamic responses of the two optimized designs to the same EC (rated wind speed) are compared in Fig. 4. The left column shows a portion of the time series of (from top to bottom): horizontal wind speed at the hub, free-surface elevation, floater surge, heave and pitch, and nacelle acceleration. The middle column shows Power Spectral Density (PSD) plots of the corresponding signals. The right column shows the exceeding probability, obtained by extracting the peaks of each time series, sorting them in ascending order and assigning an exceeding probability to each value based on its position in the list. As seen in the plots and discussed previously, the inclusion of dynamic constraints in the optimization does not seem to affect the design for the used constraint limits.

5. Final considerations

An optimization framework for floating wind turbine support structures has been adopted for the conceptual and preliminary design of the supporting structures of a reference 15 MW floating wind turbine. The framework builds on fast frequency domain analysis and analytical design sensitivities with respect to the design variables. Twelve environmental conditions of combined wind and waves were considered for optimization, and optimized design were obtained in approximately 15 min. The inclusion of additional dynamic constraints seemed to not have a

significant effect on the final design. This happened because the static constraints were governing the design, due to their tight predefined limits set in the optimization problem formulation. A relaxation of the static constraints may activate the dynamic constraints and hence lead to more marked differences between the two types of designs, i.e. designs obtained with and without the dynamic constraints. The use of harsher environmental conditions may have a similar result. A methodology for obtaining discrete optimized design solutions was proposed. The methodology builds on a post-processing phase where the continuous design is first rounded to the nearest entries in given size catalogues, and then a heuristic search is performed to explore the domain in the vicinity of the rounded solution. The methodology is proved capable of providing discrete solutions that satisfies, within acceptable limits, the problem constraints. Thus, these designs could be used as starting point for subsequent detailed design and validation phases with higher-fidelity models.

Current work is focused on extending the optimization analysis routines. The goal is to extend the problem to 3D and optimize floating wind turbine systems modelled with eight DOFs (six DOFs for the floater motion, and two DOFs for tower first fore-aft and side-side bending modes), and to be able to handle also cases with wind-wave misalignment. Moreover, the hydrodynamic sub-model is being enhanced to compute hydrodynamic properties for more complex floater geometries.

Acknowledgments

This work was carried out as part of the FloatStep project. The research leading to these results has received funding from Innovation Fund Denmark (IFD) under grant no. 8055-00075B.

References

[1] Jonkman J M 2007 Dynamics modeling and loads analysis of an offshore floating wind turbine Tech. rep. National Renewable Energy Lab., United States
[2] Fylling I and Berthelsen P A 2011 *Proceedings of the International Conference on Offshore Mechanics and Arctic Engineering - OMAE* **5** 767–776
[3] Hall M, Buckham B and Crawford C 2013 *Oceans 2013 MTS/IEEE Bergen: The Challenges of the Northern Dimension* 6608173
[4] Hall M, Buckham B and Crawford C 2014 *Renewable Energy* **66** 559–569
[5] Karimi M, Hall M, Buckham B and Crawford C 2017 *Journal of Ocean Engineering and Marine Energy* **3** 69–87
[6] Dou S, Pegalajar-Jurado A, Wang S, Bredmose H and Stolpe M 2020 *Journal of Physics: Conference Series* **1618** 042028
[7] Hegseth J M, Bachynski E E and Martins J R 2020 *Marine Structures* **72** 102771
[8] Gaertner E, Rinker J, Sethuraman L, Zahle F, Anderson B, Barter G, Abbas N, Meng F, Bortolotti P, Skrzypinski W, Scott G, Feil R, Bredmose H, Dykes K, Sheilds M, Allen C and Viselli A 2020 Definition of the IEA 15-Megawatt Offshore Reference Wind Turbine Tech. rep. International Energy Agency
[9] Jonkman J M and Jonkman B J 2016 *Journal of Physics: Conference Series* **753**
[10] Danna E, Rothberg E and Le Pape C 2005 *Mathematical Programming* **102** 71–90
[11] Pegalajar-Jurado A, Borg M and Bredmose H 2018 *Wind Energy Science* **3** 693–712
[12] Madsen F J, Pegalajar-Jurado A and Bredmose H 2019 *Wind Energy Science* **4** 527–547
[13] Morison J, Johnson J, Schaaf S *et al.* 1950 *Journal of Petroleum Technology* **2** 149–154
[14] Al-Solihat M K and Nahon M 2016 *Ships and Offshore Structures* **11** 890–904
[15] Conforti M, Cornuéjols G, Zambelli G *et al.* 2014 *Integer programming* vol 271 (Springer)
[16] Gurobi Optimization LLC 2020 Gurobi Optimizer Reference Manual version 9
[17] Allen C, Viselli A, Dagher H, Goupee A, Gaertner E, Abbas N, Hall M and Barter G 2020 Definition of the UMaine VolturnUS-S reference platform developed for the IEA Wind 15-megawatt offshore reference wind turbine Tech. rep. International Energy Agency
[18] Mahfouz Y, Salari M, Vigara F, Hernandez S, Molins C, Trubat P, Bredmose H and Pegalajar-Jurado A 2020 COREWIND D1.3: Public design and FAST models of the two 15MW floater-turbine concepts Tech. rep. University of Stuttgart